

Stiffness of FRP Pultruded Tubes under Repeated Axial Impacts

Ernesto J. Guades, Thiru Aravinthan, Md. Mainul Islam and Allan C. Manalo

Centre of Excellence in Engineered Fibre Composites, Faculty of Engineering and Surveying,
University of Southern Queensland, Toowoomba, Australia

ABSTRACT

Fibre composites in deep foundation industry have been recognized to replace conventional materials such as concrete, steel and timber in harsh marine environment. The emergence of hollow fibre reinforced polymer (FRP) composite tubes as a structural component provided the industry to consider this material as a potential composite pile type as they can carry design load. However, issue such as driving performance of this material warrants investigation as they are considered the lowest performer among composite piles. The thin-walled section generally ruptures under high driving stresses, thus its stiffness for post-impact performance is in question. This paper experimentally investigated the effects of impact energy and number of impacts on the axial stiffness of hollow FRP composite tubes. Six incident energy variants were considered, and two specimens for a given impact energy were subjected to a maximum of 130 repeated impacts using a drop-weight impact tester. The impact response and the contact stiffness were evaluated in terms of damage progression and the evolution of peak force for both collapsed and non-collapsed tubes. Results point out that no significant difference exists in the behaviour of the tubes for which no collapse occurs with test duration. On the contrary, the location of the initiation of collapse influenced the shape of the load and number of impact curves for collapsed tubes. The value of the stiffness after the initiation of collapse remains the same regardless of the magnitude of the applied energy. Furthermore on the collapsed tubes, it was observed that impact energy does not significantly reduce the stiffness of tubes during initial impacts, however, their effects were apparent as the number of impacts increases.

KEYWORD

composite piles, FRP pultruded tubes, repeated impacts, collapsed tubes, drop-weight test

1. INTRODUCTION

Fibre composite piles have been used for almost twenty five years to replace traditional materials such as concrete, steel and timber in harsh marine environment [1]. The main advantages of composites among other construction materials include lightweight, high strength-to-weight ratio, corrosion resistance, chemical and environmental resistance and low maintenance cost [2]. In Australia, the application of fibre composites in deep foundation is still in its infancy with few projects being undertaken [3].

Hollow fibre reinforced polymers (FRP) composites are now being used for pile applications as they can carry design load. Compared to concrete-filled FRP composite pile, they can be readily installed without the intricacy of placing concrete infill using additional equipments. Additionally, bond failure between the FRP shell and concrete infill is a major concern for concrete-filled FRP composite pile when loaded under pure bending [4]. However, there are problems associated with the use of hollow FRP composite piles as they are considered the lowest performer in terms of driving performance. They are susceptible to compression failure and the thin-walled section of the hollow composite pile generally shatters under high driving stresses when encountering sand layer or boulders [5]. Due to this rupture, its stiffness for post- impact performance is in question.

In this study, the axial stiffness of hollow FRP piles under driving impacts was investigated through laboratory experiment. The main objective of this work is to characterise the effect of impact energy and number of impacts on the axial stiffness of tubes relative to the use of FRP pultruded sections as hollow composite piles. The effect of non-homogeneous and anisotropic properties of soil during driving was controlled through particular testing set-up with consideration on the worst-case scenario in pile driving (i.e. when hollow FRP composite pile encounters hard soil or boulders).

Study on the behaviour of FRP tubes under repeated axial impacts are absent in the literature, however, there are few published works on the behaviour of tubes which are laterally impacted. For instance, Roy et. al. [6] characterised the loss of stiffness of carbon fibre reinforced composite tubes using swinging pendulum-type impact

fatigue tester. Micro-structural observation of this study on the fractured surfaces revealed debonding, with cracks originating in the matrix by the contact stresses. These debond cracks continue to grow in size and numbers with increasing impact cycles leading to loss of strength and stiffness.

A number of researches on impact fatigue behaviour related to composite laminates were undertaken specific for automobile and aerospace application [7-11]. In the study of Belingardi et. al. [7], they compared the response of hand lay-up and vacuum infusion glass-reinforced laminates by repeatedly impacting them up to 40 impacts or until perforation. Results showed that the stiffness of both lamination processes diminishes impact after impact and that the highest reduction is achieved in the first few impacts. This observation was also confirmed in a study of Sevkati et. al. [8] on repeated impact response of plain-woven hybrid composites. In addition to this, data points showed that the laminate stiffness is not constant at different drop heights (i.e. higher impact velocities) and the total loss of stiffness is greater for higher drop heights. It should be noted, however, that two distinctions relative to the test modes were seen between the present and the previously mentioned studies. Firstly, these research studies are impacting the composite laminate up to perforation (i.e. stiffness is zero) whilst the present study impacted the composite tube up to partial collapse (i.e. stiffness does not approach zero). Secondly, the impactor struck the laminate specimen first on the matrix with resin-rich layer; while in the present study, the impactor hit both matrix and fibre simultaneously. These distinctions were considered as they greatly influence the behaviour particularly on the stiffness degradation behaviour and on the occurrence of peak load.

2. MATERIALS AND TEST METHODS

2.1 Materials

The pultruded tubes, manufactured by Wagners Composite Fibre Technology (WCFT), Australia, are made from E-glass and vinyl ester resin. The tube wall consisted of nine plies with a total thickness of 5 mm. Starting from the exterior of the wall, the stacking sequence of the plies is in the form of $[0^0/+45^0/0^0/-45^0/0^0/-45^0/0^0/+45^0/0^0]$, where the 0^0 direction coincides with the longitudinal axis of the tube. Tables 1 & 2 show the geometric and effective mechanical properties, respectively, of the composite tubes. It should be

noted that the mechanical properties of the laminate listed in Table 2 are values along the longitudinal direction.

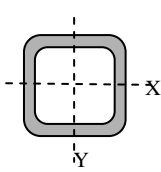


Table 1 Geometric properties

Depth	Width	Thickness
mm	mm	mm
100	100	5.25

Table 2 Coupon test results

Property	Value	Unit
Specific mass	1968	kg/m ³
Fibre fraction	77	%
Tensile strength	614	MPa
Comp. strength	510	MPa
Flexural strength	979	MPa
Modulus of elasticity	36395	MPa

2.2 Drop weight impact apparatus

Impact test was performed using un-instrumented drop weight impact testing machine defined in AS 4132.3 [12] with some modifications on the steel clamping frame to suit for the testing condition of the specimen. The impact apparatus is shown in Figure 1. The impactor is a 135 mm diameter steel cylinder with a flatted-nose contact surface and weighs up to 21.5 kg. The maximum drop height is 3 m, in which the applied energy can be varied up to 635 J.

The bottom of the tube rests on a massive concrete base to simulate the worst driving condition of hollow FRP composite pile when its toe is encountering hard soil or boulders (i.e. no advancement for several blows). The anisotropic and non-homogenous properties of soil were controlled and represented in a form of a medium fitted for this specific impact test. To attain this, polystyrene foam was inserted between the lower end of the tube and the steel frame fixture (Fig.1c). This set-up allows the tube to expand laterally during the impact regime without restraints from the frame fixture.

A 10mm thick plate was used in capping the top of the tested tube (Fig.1a- label 8). Nine slightly pre-loaded springs were attached on the steel cap and connected to the steel frame to hold the cap during rebound (Fig. 1c). During test, the impactor

is raised manually to the desired drop height through a rope attached and temporarily held and later released by an improvised clamping device positioned a distance from the impact apparatus. The rope is caught manually after each individual impact to avoid bouncing and extraneous impacts on the specimen. Steel cap is removed at least every three impacts to check the position of the impactor relative to the contact section of the tube to make sure that the tup strikes the specimen each time at approximately same location. This process is repeated until the required number of impacts on the tube was obtained.

2.3 Repeated impact testing

For repeated impact test, two impact masses and three drop heights were considered to get six incident energy variants. Two replicates with a length of 375mm for any given incident energies were subjected to a maximum of 130 impacts or up to collapse of the tubes. The detailed test matrix including some remarks and notations is provided in Table 3.

2.4 Instrumentation and data post processing

The specimen was instrumented by a shock accelerometer with model 350A14 from PCB Piezometrics, Inc. mounted on the mid-height of the tube. This accelerometer is suitable for this kind of high-strain dynamic testing as the amplitude range can reach up to $\pm 5000g$. The data acquired by the shock sensor was recorded and saved on a personal computer via LMS SCADAS Mobile data acquisition machine (see Fig. 1b) using a sample rate of 500 Hz.

The acceleration-time response curves were acquired by means of a shock sensor. The force history was calculated by multiplying the acceleration term by the impactor mass. The displacement was obtained by double integration of the acceleration and thus force-displacement curves can be plotted. The energy-displacement curves were then obtained by integration of the force-displacement curves. Trapezoidal rule was used in integration to determine velocity, displacement and energy values in Excel spreadsheets. The reliability of the test set-up and data post processing were checked by comparing both theoretical (incident energy) to the measured energy value during the 1st impact. Agreement between theoretical and measured values was found to be reasonable as the average difference for all tests is less than $\pm 3\%$.

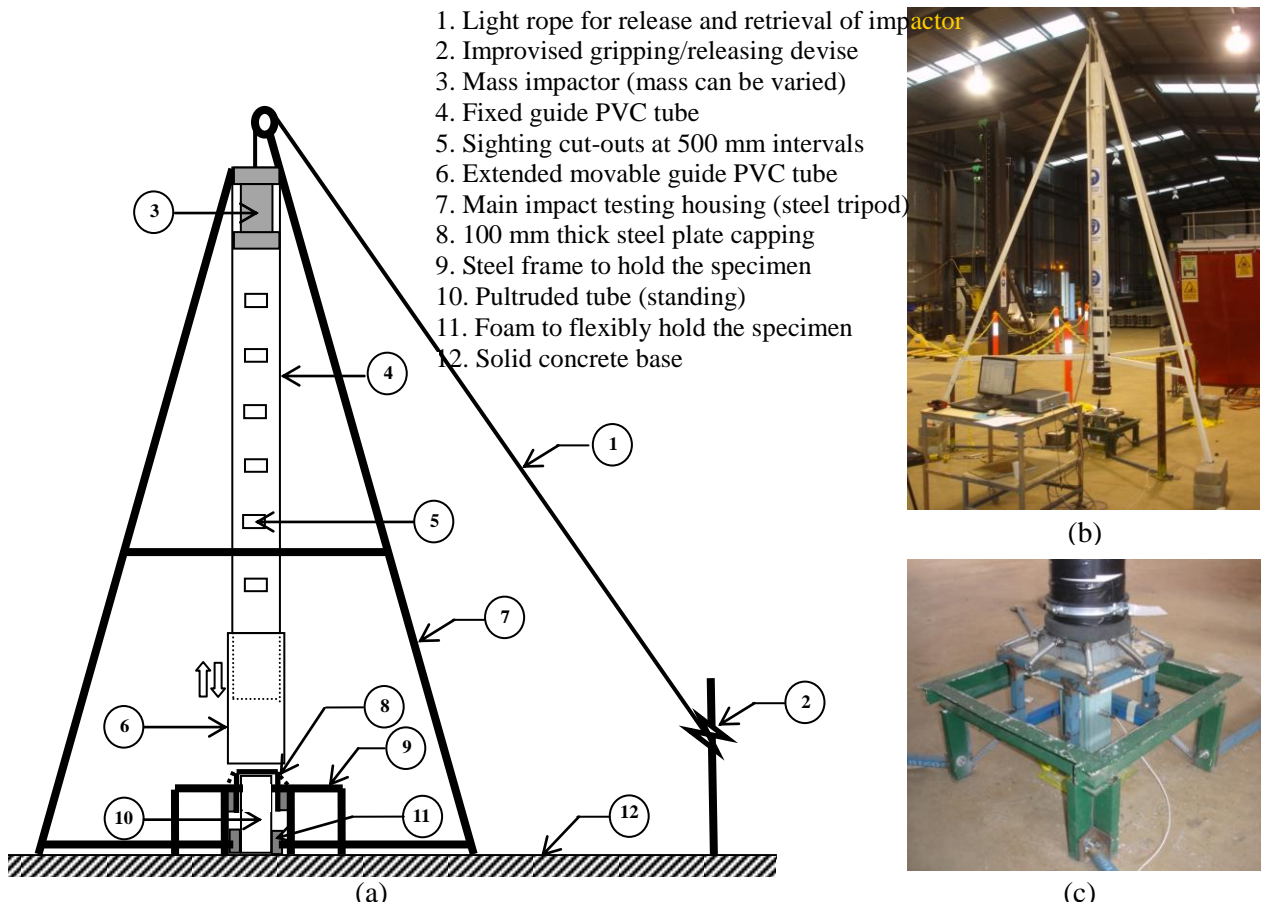


Fig. 1 Repeated impact testing. (a) Schematic diagram of drop weight impact apparatus, (b) oblique view of the impact test set-up, and (c) steel frame fixture

Table 3 Repeated impact test matrix

Specimen ID	Drop mass (kg)	Drop height (m)	Incident energy (J)	Number of impacts	Remarks
E630	21.56	3	634.51	45	*Collapsed tube
E480	16.20	3	476.77	130	Collapsed tube
E420	21.56	2	423.01	130	Collapsed tube
E320	16.20	2	317.84	130	*Non-collapsed tube
E210	21.56	1	211.50	130	Non-collapsed tube
E160	16.20	1	158.92	130	Non-collapsed tube

Note: Specimen IDs are referred from the incident energy (e.g. E630 \approx 634.51 J)

* = see Fig. 2

3. RESULTS AND DISCUSSIONS

3.1 Load-displacement relationship

Fig. 2 depicts the typical representative load-displacement curves for collapsed (E630, E480, and E420) and non-collapsed tubes (E320, E210 and E160). Whilst the slope of these curves characterises the stiffness, the enclosed area under these curves provides the total energy. For non-collapsed tubes, the 1st, 40th and 130th impacts produced very similar load-displacement curves with a negligible reduction of the peak load.

In contrary to this observation, the collapsed tubes showed an apparent drop in peak load and an increase of deformation value. A drop after an initial peak (1st impact) indicates the change of the composite from the intact to a damaged state (40th for E630 and E480, 130th for E420). The successive impacts reduced the stiffness of the tubes up to collapse as evidently observed from the curve. One comment is worthwhile making on the load-displacement plots for collapsed tubes. For E630 and E480, the behaviour of curve at the 40th impact is similar (i.e. location of peak load

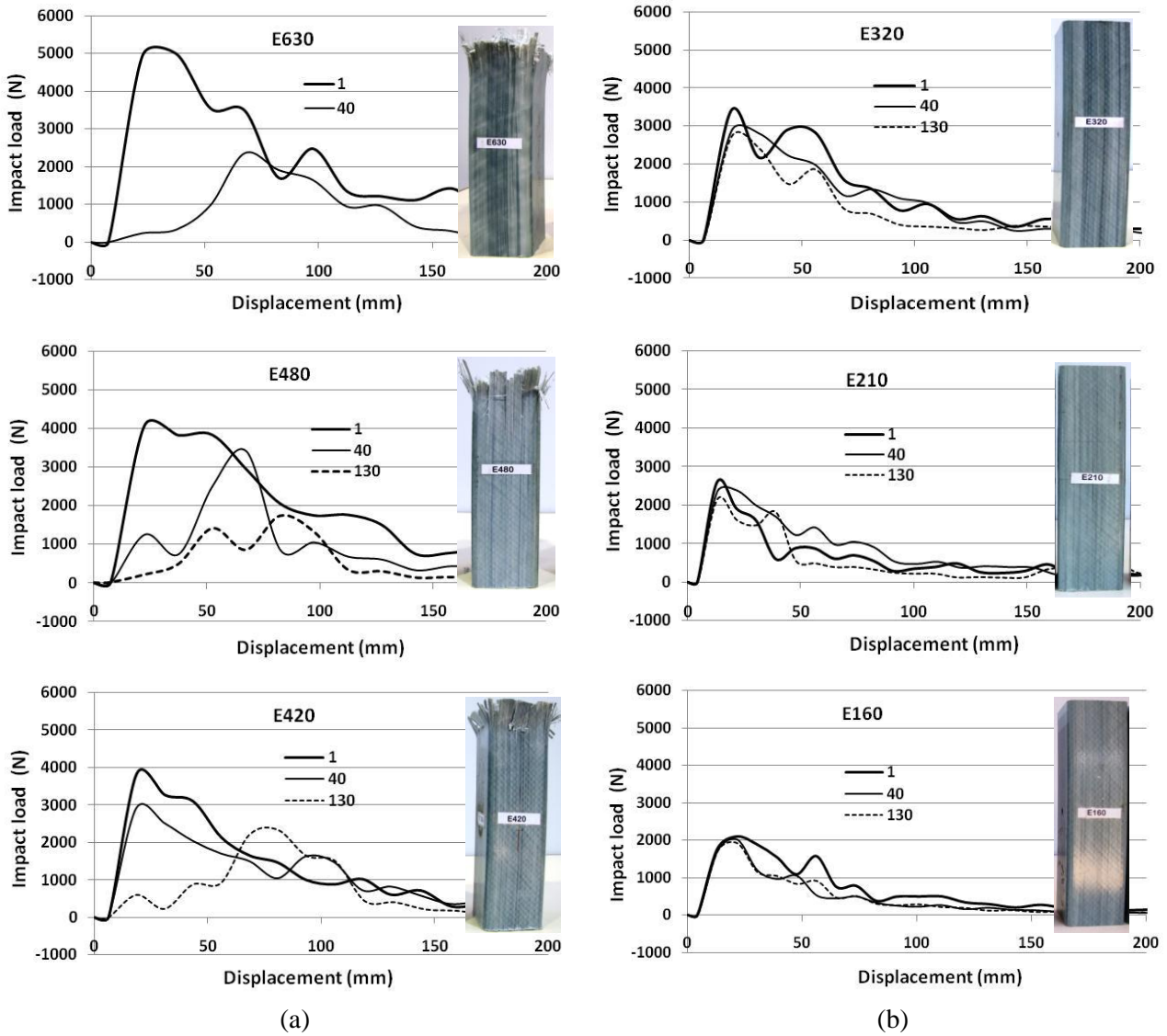


Fig. 2 Impact load versus displacement curves at 1st, 40th and 130th impacts for (a) collapsed tubes, (b) non-collapsed tubes

noticeably shifted from the 1st impact) while for E420, the location is comparable from the 1st impact. This distinction is attributed by the occurrence of the collapse initiation point (i.e. start of collapse) whereby influencing the shape of the curve. As will be discussed in the succeeding sections, the collapse initiation point for E630, E480 and E420 is approximately at the 20th, 56th and 95th impacts, respectively. For E630, 40th impact is already at the collapsed region while for E480, it is nearly close to the collapse initiation point. As a result, the behaviour is dominated by a collapse mode. In contrary, the behaviour of E420 is dominated by non-collapse mode as the location of 40th impact is a bit distant from the initiation of collapse.

3.2 Stiffness of tested tubes

Fig. 3 shows the comparison of the representative stiffness versus number of impacts curves for both collapsed and non-collapsed tubes. Experimental results presented in the figure shows that for non-collapsed tubes, the stiffness continues to slowly decrease impact after impact suggesting a slow but steady accumulation of damage. On the other hand, collapsed tubes show a reduction of stiffness on the initial impacts but reach a steady value starting from the point of collapse initiation indicating that a steady-state condition was reached. One of the notable observations that can be evinced from this figure is that for tubes repeatedly impacted up to collapse, two regions were clearly seen. The first region constituted a

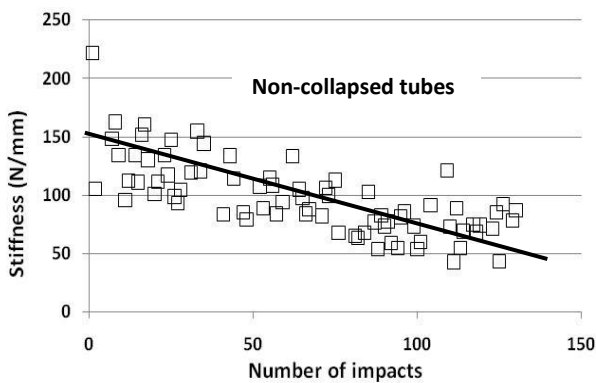
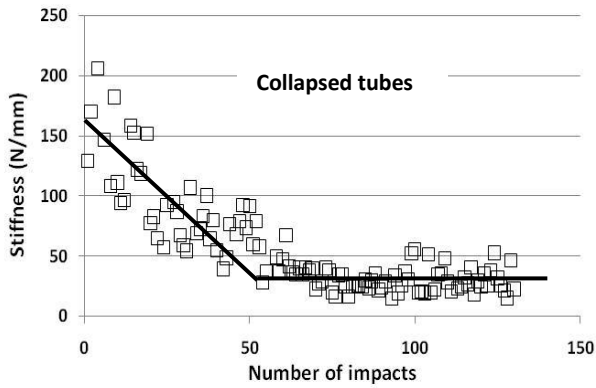


Fig. 3 Stiffness versus number of impacts for collapsed and non-collapsed tubes

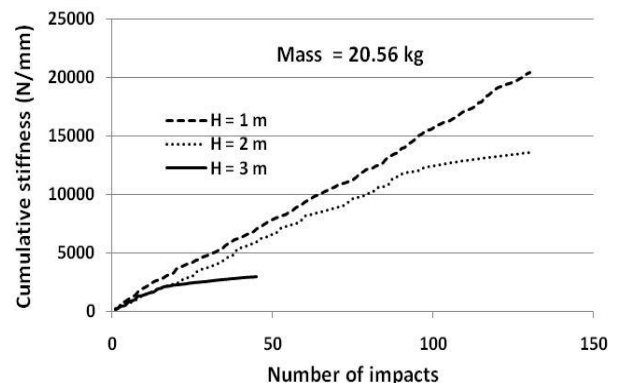
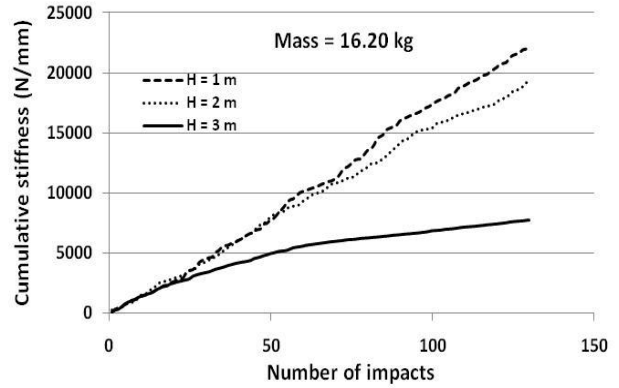


Fig. 4 Cumulative stiffness versus number of impacts for two impact masses

consistent decrease of stiffness while the second region comprised of an approximate constant stiffness value. It should be noted that the numerical value of the stiffness on the second region is not zero as the vertical crack on the corner of the tube does not extend to the bottom (see Fig. 8). Interestingly, the stiffness curve of the non-collapsed tubes is only one part of a region (i.e. first region) for collapsed tubes.

3.3 Variation of stiffness with impact mass

The relationship between the cumulative stiffness and number of impacts curves for two impact masses adopted is shown in Fig 4. Data point on the figure show that the tube stiffness is not constant at different drop heights. The stiffness of the tube decreases impact after impact regardless of the impact masses. It should be noted that the turning point on the graph (i.e. 20.56 kg at 2 and 3 m drop heights, and 16.20 kg at 3 m) indicates the start of collapse of the tubes. No clear trend of the stiffness ratio deviation between drop heights for both impact masses was observed. However, the number of impacts in which the curves intersect

can be visibly identified. The number of impacts in which the cumulative stiffness overlaps with each other at different drop heights is approximately 20 and 5 for a drop mass of 16.20 and 20.56 kg, respectively. The difference in number of impacts points out that the decrease in the stiffness of the tube is more significant for higher impact mass.

3.4 Comparison of stiffness of collapsed tubes

Fig. 5 evinces the comparison of cumulative stiffness versus number of impacts for collapsed tubes. As previously discussed, the turning point on the graph (A, B and C) indicates the start of collapse of the tubes. The number of impacts to initiate collapse is from 18-22, 53-59 and 93-97 for E630, E480 and E420, respectively. However, average value (i.e. 20, 56, and 95, respectively) will be used in further discussions. It was observed from the figure that the cumulative stiffness curves initially coincides up to 10 impacts and finally departs until permanent collapse. This observation suggests that the effect of incident energy was apparently seen to be more damaging after these

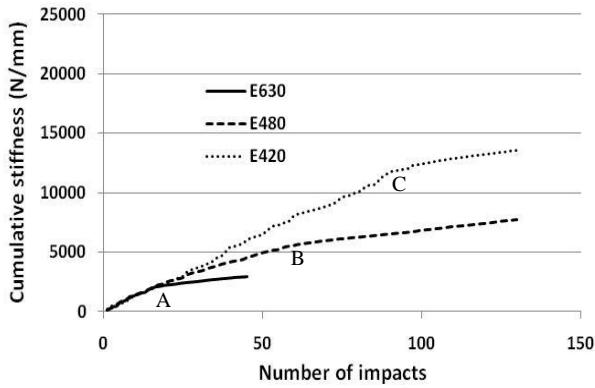


Fig. 5 Cumulative stiffness versus number of impacts for collapsed tubes

initial impacts regime. Additional scrutiny that can be generated from this curve is the location of the collapse initiation (i.e. impact number) in which it decreases with increasing incident energy. The reduction in the impact number to collapse the tube suggests that higher impact energies are more devastating than lighter impacts. This general finding was also supported by the study conducted by Belingardi et al [7] and Sevkat et al. [8] on laminate impact test.

3.5 Stiffness comparison of tubes after initiation of collapse

The correlation between the stiffness and relative number of impacts at the initiation of collapse is shown in Fig. 6. It should be emphasized that the relative number of impacts is the number of impacts measured from the initiation of collapse (Point A, B and C) to the total impacts the tube has experienced (45, 130, 130 for E630, E480 and E420, respectively).

Interestingly, no significant difference on the stiffness was observed on the graph with different incident energies. This phenomenon can be explained by illustrating the relationship between the incident energy, the energy measured at the mid-height (no damage) and energy computed at the top of the tube (damaged portion) which is illustrated in Fig. 7. It should be noted that the obtained value from the mid-height is the average value of energy after the initiation of collapse up to the maximum cycle the tube has impacted. The energy value at the top of the tube was computed by subtracting the incident energy by the energy measured at the mid-height. As can be seen from this figure, the measured energy at the mid-height

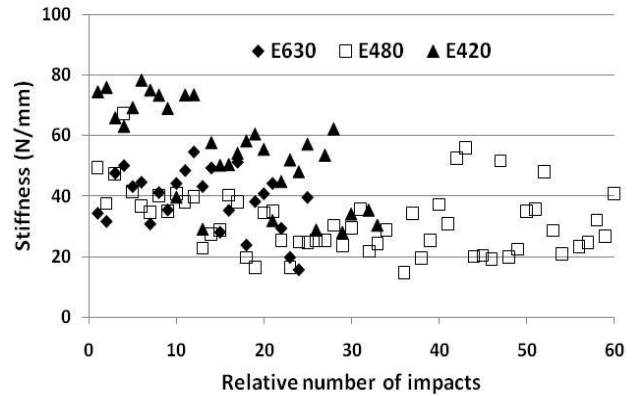


Fig. 6 Stiffness versus number of impacts curve after the initiation of collapse

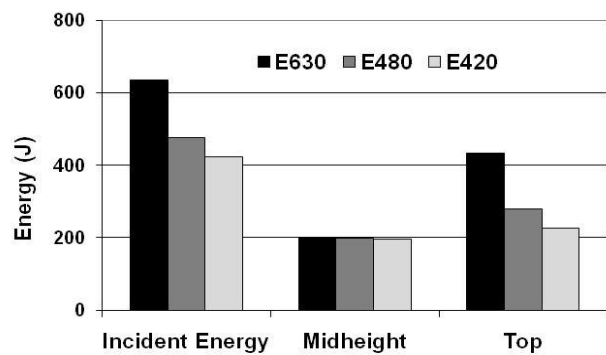


Fig. 7 Bar chart comparison of energy for the collapse tubes



Fig. 8 Snapshot of collapsed tubes indicating damaged heights

is same regardless of the applied energy. This implies that for non-damage portion of the tube, the stiffness is no longer affected or reduced as all of the applied energy are fully absorbed by the damaged portion (top) as seen from graph (see energy measured at the top of the tube). The different applied energy demand is therefore

constantly absorbed at the undamaged portion (mid-height) but increasingly absorbed at the damaged portion (top). This is manifested in the graph as the energy at the top increases with increasing incident energy.

The absorption behaviour on the damaged portion of the tube can be also characterised by the damaged height (H_d) propagation shown in Fig. 8. The measured damaged height for E630, E480 and E420 is 55, 35 and 5 mm, respectively. The increase in the damaged heights explains alternatively that smashed portion of the tube is increasing with increasing applied energy.

4. CONCLUSIONS

The stiffness of hollow FRP pultruded tubes was investigated using repeated axial impact. The contact stiffness was evaluated in terms of damage progression and the evolution of peak force for both collapsed and non-collapsed tubes. Based from the findings of this study, the following conclusions were drawn.

- (1) No significant difference exists in the load-deformation curve for tests in which no collapse occurred
- (2) The load-displacement curve is influenced by the location of the initiation of collapse
- (3) The stiffness of the tube decreases under repeated impact and the reduction is more pronounced for higher impact mass.
- (4) In general, impact energy does not significantly reduce the stiffness of tubes during initial impacts, however, their effects were apparent as the number of impacts increases.
- (5) The stiffness of collapsed tubes after the initiation of collapse remains the same regardless of the magnitude of the applied energy.

ACKNOWLEDGEMENT

The authors gratefully acknowledged Wagners Composites Fibre Technology (WCFT), Toowoomba, Australia, for providing samples in the impact test. Acknowledgment is also given to Mr. Wayne Crowell for helping in the conduct of experiment.

REFERENCES

- [1] M. G. Iskander and M. Hassan: State of the practice review in FRP composite piling, ASCE Journal of Composites for Construction, pp. 116 - 120, August 2005.
- [2] M. Sakr, M.H. El Naggar and M. Nehdi: Interface characteristics and laboratory constructability tests of novel fibre-reinforced polymer/concrete piles, ASCE Journal of Composites for Construction, pp. 274 - 283, May - June 2005
- [3] E. J. Guades, T. Aravinthan and M. Islam: Driveability of composite piles: Proceedings of the 1st International Postgraduate Conference on Engineering, Designing and Developing the Built Environment for Sustainable Wellbeing, QUT, Brisbane, Australia, pp. 237-242, April 27-29, 2011.
- [4] A. Mirmiran, M. Shahawy, C El Khoury and W. Naguib: Large beam-column tests on concrete-filled composite tubes, ACI Structural Journal, Vol. 97, pp. 268 - 277, March - April 2000.
- [5] A. Mirmiran, Y. Shao and M. Shahawy: Analysis and field tests on the performance of composite tubes under pile driving impact, Composite Structures, Vol. 55, pp. 127 - 135, 2002.
- [6] R. Roy, B.K. Sarkar and N.R. Bose: Impact fatigue of glass fibre-vinylester resin composites, Composites:Part A, Vol. 32, pp. 871 - 876, 2001.
- [7] G. Belingardi, M. Cavatorta, and D. Paolino: Repeated impact response and hand lay-up and vacuum infusion thick glass reinforced laminates, International Journal of Impact Engineering, Vol. 35, pp. 609 - 619, 2008.
- [8] E. Sevkat, B. Liaw, F. Delale, and B. Raju: Effect of repeated impacts on the response of plain-woven hybrid composites, Composites:Part B, Vol. 41, pp. 403 - 413, 2010.
- [9] B.P. Jang, W. Kowbel and B.Z. Jang: Impact behaviour and impact-fatigue testing polymer composites, Composites Science and Technology, Vol. 44, pp. 107 - 118, 1992.
- [10] B.S. Sugun and R.M. Rao: Low-velocity impact characterization of glass, carbon and Kevlar composites using repeated drop tests, Journal of Plastics and Composites, Vol. 23, pp. 1583 - 1599, 2004.
- [11] M.S. Found, and I.C. Howard: Single and multiple impact behaviour of a CFRP laminate, Composite Structures, Vol. 32, pp. 159 - 163, 1995.
- [12] Australian Standards 132.3.: Australian standard on boat and ship design and construction, Part 3: Fibre-reinforced plastics construction, 1993.